Journal of Sol-Gel Science and Technology 8, 285–291 (1997)

Influence of Cd Content and Se Doping on the Formation of CdSe Nanocrystals in Silica Xerogels: A SAXS Study

D.A. HUMMEL AND I.L. TORRIANI
Instituto de Física Gleb Wataghin, UNICAMP, Campinas, S.P., Brazil

A.F. CRAIEVICH
Laboratório Nacional de Luz Síncrotron/CNPq, Campinas, S.P. and Instituto de Física/USP, São Paulo, S.P., Brazil

N. DE LA ROSA FOX
Instituto de Física, Universidad de Cádiz, Puerto Real, Cádiz, Spain

A.Y. RAMOS
LMCP/CNRS, Université de Paris VI, Paris, France

O. LYON
LURE/CNRS, Université Paris-Sud, Orsay, France

Abstract. Small-angle X-ray scattering (SAXS) experiments were carried out to characterize the structure of the composite formed by CdSe nanocrystals embedded in a porous silica matrix (silica xerogels containing Cd with formamide addition and ultrasound treatment). SAXS results from samples before Se diffusion indicate the presence of heterogeneities with a bimodal size distribution which was associated to the existence of mesopores (pores of several hundred Å) immersed in a nanoporous matrix (characteristic pore radii of 20–30 Å). The diffusion of Se induces the nucleation and growth of CdSe nanocrystals. The average size of the nanocrystals increases with Cd content. Higher Se doses promote the formation of larger nanocrystals (radius of gyration of ∼30 to 50 Å). Anomalous scattering results confirm the existence of Se aggregation associated with CdSe nanocrystal formation and suggest that only partial segregation of Cd and Se occurs.

Keywords: CdSe nanocrystals, silica xerogels, sonogels, SAXS

1. Introduction

Silicon alkoxide-derived sonogels have particular microstructural characteristics induced by both the solventless processing and the cavitation phenomenon in the alkoxide-water mixture. Unique features of sonogels include short gelation times and high bulk density with very fine and uniform porosity [1]. Finely dispersed nanocrystalline particles embedded in a dielectric silica matrix behave as quantum dots, producing the confinement of discrete excitons and leading to a non-linear optical response and an intensity-dependent refractive index [2]. Silica is an excellent matrix for the composites, since it has a wide band-gap energy and the confinement effect of the embedded semiconductor nanocrystals is very pronounced, acting as a true potential well. Assuming that nanocrystals are nucleated at the nanopores, a matrix containing a dense and fine porosity would give rise to a high population of nucleation centers and promote the formation of nano-sized crystals [3].

Previous studies have shown that the combined effect of the addition of formamide as a drying control agent in the sol and the action of high-power ultrasound for gelation permits the tailoring of desired specific matrix structures [1, 4]. Chalcogenides (CdS, CdSe, CdTe, etc.) are often chosen as dopants because they can easily be prepared by chemical precipitation at room temperature, have high values of third-order susceptibility and exhibit short switching times [2].

The purpose of this paper is to characterize the structure of the composite material silica xerogel-nanocrystalline CdSe. The influence of Cd^{+2} content and Se^{-2} diffusion dose on the structure is determined using the classical SAXS technique. Anomalous SAXS is utilized to selectively study the CdSe nanocrystal formation.

2. Experimental

Silica sonogel matrices were prepared from TEOS + water (pH = 1) + formamide in a molar ratio of 1 : 10 : 7 as described previously [3]. Cd^{+2} ions were incorporated by adding $\mathrm{Cd(NO_3)_2}$ to the hydrolysis water. Concentrations were 1, 5 and 10 wt.% of final Cd^{+2} content in the silica matrix in order to obtain the composite $(\mathrm{SiO_2})_{100-x} - (\mathrm{CdSe})_x$, where $x = 1$, 5 and 10, respectively. The samples (labeled M1, M5 and M10) were placed in identical hermetic polyethylene containers and maintained at a constant temperature (40°C) until gelation occurred. The gels were then aged during three days, when the containers were opened to partially evaporate the syneresis liquid. One additional step was the impregnation of the resulting gels, dipping them in a sol of the same starting composition under vacuum conditions. At this point the silica matrices were ready for Se^{-2} diffusion.

Se^{-2} ions were diffused in the samples using KSeCN water solutions with concentrations of 5.10^{-3} M and 5.10^{-4} M. The resulting samples will be henceforth designated (H) and (L) for high and low Se^{-2} diffused dose, respectively. The doped gels resulting from the 1, 5 and 10% wt. Cd^{+2} content were labeled L1, L5, L10, respectively, for low Se^{-2} diffused dose, and H1, H5 and L10 for high Se^{-2} diffused dose. All gels were red coloured, suggesting the formation of CdSe crystals. In order to improve their optical quality and structural stability, the samples were still submitted to an impregnation process, keeping them under vacuum for one hour and then dipping them in the corresponding starting solution for a period of 24 hours. After washing the gels with distilled water in order to remove any remaining residues, they were dried in an oven at 40°C.

The SAXS experiments were carried out using the D22 synchrotron radiation workstation at LURE, Orsay. The experimental setup is composed of a double-crystal monochromator which provides a monochromatic and tunable X-ray beam. The intensities were determined as a function of the modulus of the scattering vector $q = 4\pi \sin\theta/\lambda$, θ being half of the scattering angle and λ the X-ray wavelength.

Two types of experimental studies were carried out: (i) classic SAXS using 8.048 and 12.505 keV photons and two sample detector distances to record the scattering intensity in the small ($0.003\ \mathrm{\AA}^{-1} < q < 0.03\ \mathrm{\AA}^{-1}$) and large ($0.02\ \mathrm{\AA}^{-1} < q < 0.40\ \mathrm{\AA}^{-1}$) q-regions, respectively, and (ii) anomalous SAXS over a range of photon energies close to the Se K-edge ($E = 12.6540$ keV). The classic SAXS measurements were performed on three sets of xerogel samples containing 1, 5 e 10% Cd^{+2} content, each of them without Se^{-2} diffusion and with low and high Se^{-2} diffused dose. The SAXS study was performed in the range $0.01\ \mathrm{\AA}^{-1} < q < 0.18\ \mathrm{\AA}^{-1}$ using five photon energies close to the selenium K-edge ($E = 12.606$ keV) for a sample containing 5% Cd with high selenium dose. Before analysis, the experimental data were corrected from parasitical scattering by subtraction of a constant background and normalized to an equivalent intensity of the incident beam.

3. Results and Discussion

Scattering curves in log-log scale from gels with 5% of Cd^{+2} content are plotted in Fig. 1. SAXS results corresponding to samples without Se^{-2} diffusion (M5) and with low (L5) and high (H5) Se^{-2} diffused dose are presented. The scattering curves corresponding to samples M5 and L5 exhibit a similar behavior. They have a quasi-linear decrease below $\log q = -2.2$, a shoulder between -2.0 and -1.0 and another linear decrease for $\log q > -0.8$.

At high q, a linear behavior in $\log I(q)$ vs. $\log q$ plots indicates a power q-dependence:

$$I(q) \propto q^{-a} \qquad (1)$$

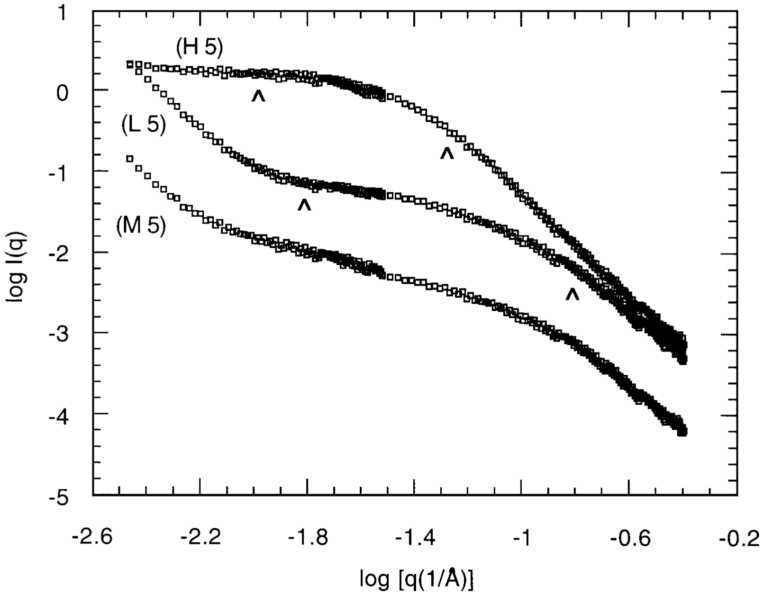

Figure 1. Log-log plots of SAXS intensities from xerogels containing 5% Cd^{+2}, without Se^{-2} diffusion (M5), with low Se^{-2} diffusion (L5) and with high Se^{-2} diffusion (H5). Since curve M5 is similar to L5, it was vertically displaced (-1) for clarity. The three curves were normalized to equivalent intensity of the incident X-ray beam and equivalent sample absorption. The gyration radii corresponding to L5 and H5 samples were determined using the q-range between arrows. (No clear linear behaviour in Guinier plots was observed for M5 samples).

In the case in which Porod's law applies (two electron density system with sharp interfaces), the exponent $a = 4.0$ [5]. This behavior is expected in the high-q limit, within a large q-range which depends on the coarseness of the structure. Other exponents are predicted for different structures such as fractal structures or non-perfect two electronic density systems in which one of the phases contains density fluctuations.

If the scattering object is composed of a nearly homogeneous matrix in which a minority fraction of isolated nanopores or nanocrystals are immersed, Guinier's equation holds and can be used to determine an average radius of gyration, R_g, of the scattering centers:

$$I(q) = N\langle V^2\rangle(\rho - \rho_0)^2 \exp\left(1/3R_g^2q^2\right) \qquad (2)$$

where N and $\langle V^2\rangle$ are the number and average of the squared volume of the particles, respectively, and $(\rho - \rho_0)$ is the difference in electronic density between particles and matrix. Guinier's equation applies to the small q range ($q < 1/R_g$).

The SAXS intensity corresponding to the xerogel before Se^{-2} diffusion with 5% Cd^{+2} content (M5 sample) is plotted in Fig. 1. The sharp decrease at small q and the shoulder in the central q range of SAXS intensity were attributed to the existence of a bimodal porosity. The feature of the SAXS curve at low q would be produced by large mesopores and the shoulder by nanopores. The fast decrease in SAXS intensity at small q, corresponding to the coarse mesoporosity, is also apparent in SAXS curves corresponding to samples containing 1 and 10% Cd^{+2} (M1 and M10 in Fig. 1).

In the central part of the scattering curve corresponding to sample M5, a Guinier average radius of 20 Å is obtained for the nanopores. The assymptotic slope of the high-q region of curve M5 in Fig. 1 is equal to 3.5, which is lower than the value expected from Porod's law. The deviation from Porod's law may be due to a contribution to SAXS intensity from electronic density fluctuations in the matrix. This contribution is expected to be significant because the matrix has not a rigorously constant electronic density and the nanocrystals occupy only a small fraction of the total volume.

Figure 1 also displays the SAXS intensity corresponding to the low and high Se^{-2} diffused samples (L5 and H5, respectively). The optical properties of both Se^{-2} diffused samples indicated that CdSe nanocrystals were formed. On the other hand, the shape of curves L5 and M5 are similar, indicating that

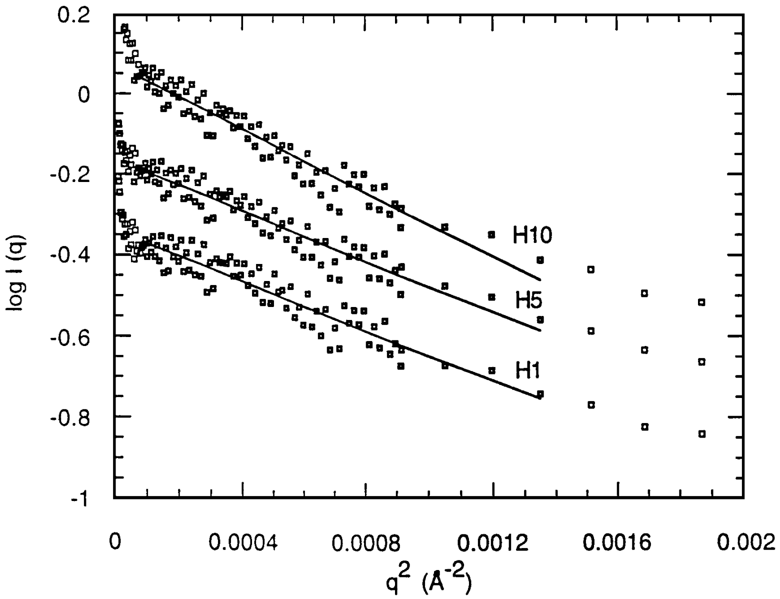

Figure 2. Guinier plots corresponding to gels with high Se^{-2} diffusion containing 1% Cd^{+2} (H1), 5% Cd^{+2} (H5) and 10% Cd^{+2} wt.% (H10) of final CdSe in the silica matrix. Note the intensity increase in the low-q region.

the scattering entities have similar sizes in the two cases. Therefore, we conclude that L5 samples exhibit a coarse structure composed of mesopores (sizes of hundreds of Å) and a fine structure composed of nanopores and nanocrystals, both with average radii of gyration of the order of 30 Å. The curve H5 is clearly different when compared with M5 and L5. Since at small q no significant contribution from the coarse porosity is apparent in H5, we concluded that SAXS intensity from high Se^{-2} diffused dose samples is almost totally due to its fine structure. This result suggests that high Se^{-2} diffused dose promotes a much more efficient process of CdSe nanocrystal formation and growth. As stated in Eq. (2), the increase in SAXS intensity from high Se^{-2} diffused dose samples may be due to an increase in (i) number of nanocrystals N, (ii) average squared volume of nanocrystals $\langle V^2 \rangle$ and/or (iii) electronic density contrast $(\rho - \rho_0)$ between nanocrystals and matrix.

The SAXS curves corresponding to the sets of samples M1, L1, H1 (low Cd^{+2} content) and M10, L10, H10 (high Cd^{+2} content) exhibit shapes qualitatively similar to the set M5, L5, H5 plotted in Fig. 1. This indicates, also for these samples, the coexistence of a coarse structure (several hundreds of Angströms) and a fine structure (a few tens of Angströms) associated with mesopores and nanopores/nanocrystals, respectively. Consequently, the nanostructure of the samples studied seems to be independent of the initial cadmium content.

We applied Eq. (2) in order to determine the average size of the CdSe nanocrystals and its dependence with Cd^{+2} content and Se^{-2} diffused dose. Scattering curves corresponding to the H1, H5 and H10 samples are presented in Fig. 2 as $\log I(q)$ vs q^2 plots. Guinier radii were obtained from least square regressions in the linear parts. The size of the mesopores are estimated as several hundred Angströms from the asymptotic behaviour in the low region of the curve (before the shoulder). The average radii of gyration, R_g, of the CdSe nanocrystals are plotted in Fig. 3. These values of Guinier radii indicate that, for a given Cd^{+2} concentration, higher Se^{-2} diffused dose promotes the formation of larger nanocrystals (radii of gyration from 35 to about 50 Å). For samples with low selenium diffusion dose, a slight increase in nanocrystal size is apparent for increasing Cd^{+2} content. This increase also occurs and is more pronounced for high Se^{-2} diffused dose (from 45 to 52 Å).

In a previous study of a similar xerogel containing 1% Cd^{+2} content, it was observed that the radius of gyration of the nanoparticles decreases for increasing Se^{-2} diffused dose [3]. In the present investigation, the Guinier radius of the nanocrystals was found to have an

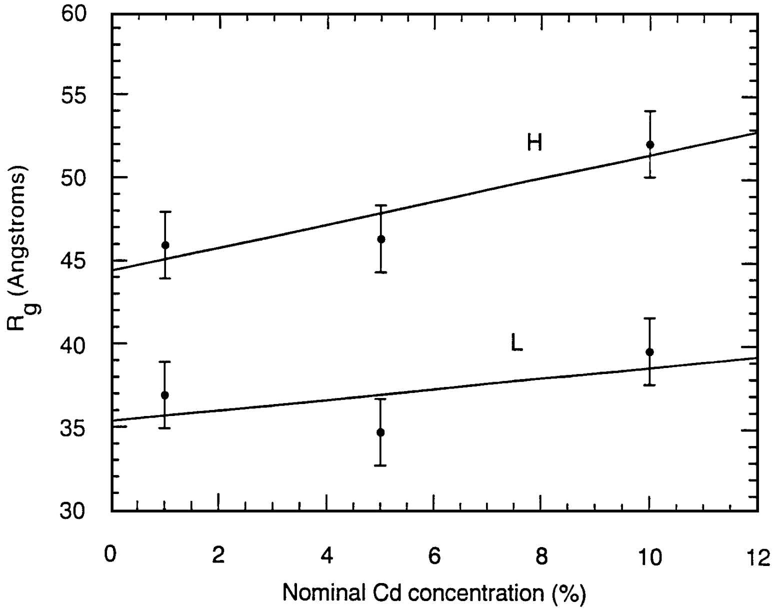

Figure 3. Guinier radii corresponding to gels with low (L) and high (H) Se^{-2} diffused dose as functions of Cd^{+2} concentration.

opposite behavior (Fig. 3). This inconsistency may be associated to differences between the efficiency of the impregnation process used for the set of samples studied in the previous investigation and in the present one. This would imply that Se^{-2} diffusion for nanocrystal formation is very sensitive to the extent of porosity filling. It should be stressed, as can be seen in Fig. 3, that the higher size of CdSe nanocrystals for higher Se^{-2} diffused dose was an effect clearly apparent, in the present investigation, for the three Cd^{+2} compositions (1, 5 and 10%).

We carried out anomalous scattering measurements in order to confirm that a fraction of the total SAXS intensity recorded at a fixed energy is actually due to a segregation process. The purpose was to check that, when Se^{-2} is diffused, the variations observed in SAXS intensity are not totally associated with eventual changes in the structure of the nanoporosity of the studied xerogel. A SAXS takes advantage of the large energy dependence of the scattering factor f' near the absorption edge of a given element. The presence of this element in the scattering entities yields differences in the scattering intensities for different energies of the incident photons close to the absorption edge ("anomalous effect"). In the present case, the existence of an anomalous x-ray scattering effect close to the Se edge, at small q, would imply that there is a Se segregation in the sample, this fact being consistent with CdSe nanocrystal formation.

Even though the SAXS intensities are not measured in an absolute scale, it is possible to determine the molecular density ratio, η, between the segregated zones (nanocrystals) and the matrix. This can be done using the procedure described by Goericgk et al. [6]. The molecular density ratio is then given by:

$$\eta = F_m[f_{0,\mathrm{Cd}} + f_{0,\mathrm{Se}} - (b/a)/(0.96)]^{-1} \tag{3}$$

where $f_{0,\mathrm{Cd}}$ and $f_{0,\mathrm{Se}}$ are the normal scattering factors of Cd and Se, respectively, F_m is approximately the scattering factor of the SiO_2 molecules. Neglecting second order factors, the energy dependence of the intensity can be expressed in the simplified form:

$$[I(E)_q]^{1/2} = a_q F'_{\mathrm{CdSe}}(E) + b_q, \tag{4}$$

which holds for any value of q. The parameter F'_{CdSe} depends on the anomalous contribution to the atomic scattering factors for Cd and Se in the crystalline particles [6].

The five experimental SAXS functions, corresponding to different energies, were corrected for the effects of different sample absorption and detector efficiency. The normalized SAXS functions are plotted in Fig. 4.

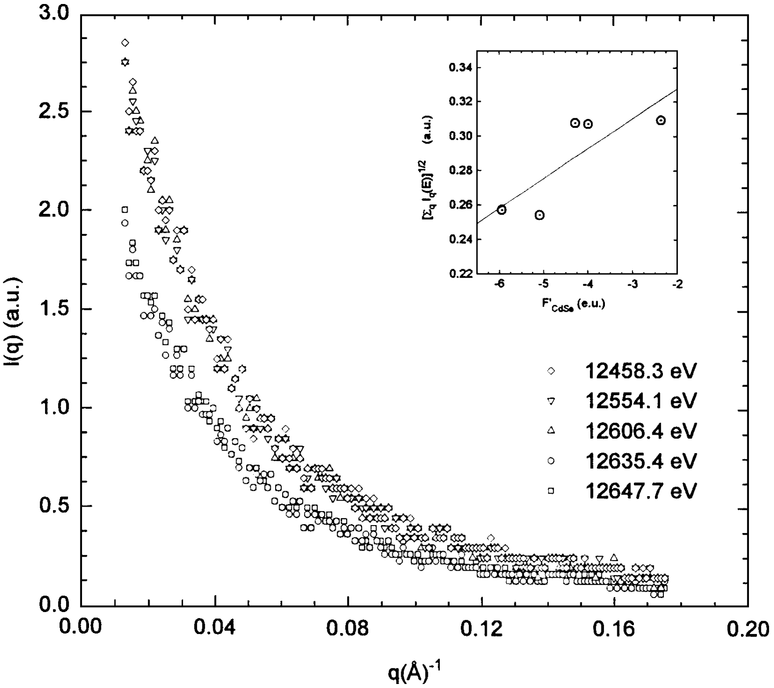

Figure 4. SAXS intensity plots corresponding to gels with 5% Cd^{+2} content and high Se^{-2} diffused dose obtained at different photon energies. Inset: $[I(0)]^{1/2}$ vs. $F'(E)$ plot.

In order to minimize statistical errors, Eq. (4) was applied to the sum of the scattering intensities within a determined q range. In our case we used the interval $0.01\ \mathring{A}^{-1} < q < 0.10\ \mathring{A}^{-1}$, in which the SAXS intensity is significant and the contribution of the coarse porosity is low. Therefore, the quotient b/a was obtained from the plot of $[\sum_q I(E)]^{1/2} = aF'_{\mathrm{CdSe}}(E) + b$. Using the experimental values of $[\sum_q I(E)]^{1/2}$ and $F'_{\mathrm{CdSe}}(E)$ from data of Ref. [7], the result presented in the inset of Fig. 4 was obtained. The coefficients a and b of the straight line were determined by least square fitting. Substituting (b/a) in Eq. (3), a value for the ratio between the molecular concentration in the nanocrystals and matrix, $\eta = 0.50$, was obtained.

An independent estimate of the parameter η was obtained assuming the nanocrystals as having the same electronic density of bulk crystalline CdSe ($n_p = 1.46$ e/$\mathring{A}^3$) and the matrix having the electronic density of amorphous silica ($n_m = 1.0$ e/$\mathring{A}^3$). These assumptions lead to $\eta = 0.80$. The rather low value of the experimental parameter η(=0.50) may be due to an incomplete segregation of Cd and Se, which would reduce significantly the contrast in electronic density between CdSe crystals and matrix. A similar value for η(=0.50) was obtained in a recent investigation of CdSe formation in homogeneous silica-based glasses [6].

Conclusions

This study demonstrates that silica sonogels exhibit, in addition to the nanoporosity detected in previous investigations [3], a coarse mesoporosity. This mesoporosity was detected in pure xerogels and also in gels containing CdSe nanocrystals.

The size of CdSe nanocrystals increases for increasing Se^{-2} diffused dose. On the other hand, higher Cd^{+2} content promotes the formation of larger nanocrystals, thus reducing the scattering contribution from the mesopores. This influence is stronger for high Se^{-2} diffused dose gels. The anomalous SAXS results are consistent with the assumption of CdSe nanocrystal formation and suggest that only partial segregation of Cd and Se occurs.

A comparison of the present results with those of a previous investigation [3] suggests that the microstructure of the studied xerogels depends critically on the impregnation process, which stops the gel evolution.

Therefore, a careful characterization of the optimal impregnation process seems to be necessary in order to control the final microstructure. This would help in the obtention of CdSe-doped gel composites with especially designed non linear optical properties.

Acknowledgments

The present work was sponsored by the Conselho Nacional de Pesquisas/CNPq (Brazil) and the Instituto de Cooperación Iberomericano (Spain).

References

1. N. de la Rosa Fox, L. Esquivias A.F. Craievich, and J. Zarzycki, J. of Non-Cryst. Solids **121**, 211 (1990).
2. R.K. Jain and R.C. Lind, J. Opt. Soc. Am. **73**, 647 (1983).
3. D.C. Hummel, I.L. Torriani, A.Y. Ramos, A.F. Craievich, and N. de la Rosa Fox, Mat. Res. Soc. Symp. Proc. **346**, 673 (1994).
4. L.L. Hench, in *Science of Ceramic Chemical Processing*, edited by L.L. Hench and D.R. Ulrich (Wiley, N.Y., 1956), p. 52.
5. A. Guinier and G. Fournet, *Small Angle Scattering of X-Rays* (Wiley, N.Y., 1955).
6. G. Goerigk, H.G. Haubold, C. Klingshirn, and A. Uhrig, J. of Applied Cryst. **27**, 907 (1994).
7. S. Sasaki, KEK Report 88-14, 1989 M/D.